



# The effect of Cu addition on the hot deformation behavior of NiTi shape memory alloys

M. Morakabati<sup>a</sup>, Sh. Kheirandish<sup>a,\*</sup>, M. Aboutalebi<sup>a</sup>, A. Karimi Taheri<sup>b</sup>, S.M. Abbasi<sup>c</sup>

<sup>a</sup> Center of Excellence for Advanced Materials and Processing (CEAMP), School of Metallurgical and Materials Engineering, Iran University of Science and Technology (IUST), Tehran, Iran

<sup>b</sup> Department of Materials Science and Engineering, Sharif University of Technology, Tehran, Iran

<sup>c</sup> Advanced Materials Research Laboratory, K.N. Toosi University of Technology, Tehran, Iran

## ARTICLE INFO

### Article history:

Received 17 November 2009

Received in revised form 21 January 2010

Accepted 22 January 2010

Available online 2 February 2010

### Keywords:

Hot deformation

NiTi alloy

NiTiCu alloys

Dynamic restoration processes

## ABSTRACT

The influence of Cu addition on the hot deformation behavior of NiTi shape memory alloys was investigated using hot compression test. A series of alloys with different Cu contents of  $\text{Ti}_{50.4}\text{Ni}_{49.6-x}\text{Cu}_x$  ( $x = 0, 3, 5, 7$  at.%) were deformed under compression to a true strain of 0.7 at the temperature range of 700–1000 °C with 100 °C intervals and constant strain rate of  $0.1 \text{ s}^{-1}$ . The stress–strain curves showed that the addition of Cu to NiTi alloy made the flow curves shift upward. This was confirmed by the calculated critical stress,  $\sigma_c$ , obtained from inflections in  $\theta$ – $\sigma$  plots, which is attributed to the formation of high strength Cu containing precipitates and solid solution hardening caused by substitution of Cu for Ni. It was also found that the maximum softening rate,  $\dot{\varepsilon}^*$ , obtained from  $\theta$ – $\dot{\varepsilon}$  plots, was increased by increasing Cu content. The microstructural analysis showed the evidence of dynamic recovery by revealing the elongated and serrated grain boundaries at 800 °C. However, a few dynamic recrystallized grains were found at this temperature. On the other hand, grain growth was also seen at 1000 °C.

Crown Copyright © 2010 Published by Elsevier B.V. All rights reserved.

## 1. Introduction

NiTi shape memory alloys have been widely used in different fields of aerospace and medicine because of superior shape memory effect and higher super-elasticity compared to other shape memory alloys [1–3]. The shape memory properties of NiTi alloys can be modified by adding ternary elements which are chemically similar to Ni or Ti [4]. The substitution of Cu for Ni can narrow the transformation hysteresis, reduce the chemical composition dependency of transformation temperatures, and improve the actuation response and fatigue properties. Therefore, NiTiCu alloys are actually beneficial for many applications such as actuators [5–8].

Since the properties of NiTi alloys are significantly affected by thermomechanical treatments, the research studies have been directed to investigate the thermomechanical behavior of these alloys [9,10]. Most of the studies carried out on thermomechanical treatment of NiTi alloys have dealt with the effects of marforming [10,11], ausforming [12,13], cold rolling and annealing [14,15], and various severe plastic deformation processes on the shape memory properties [13,16].

Primary studies on the hot deformation of NiTi based alloys have been performed by Lin and Wu [17] in which they have investi-

gated the effect of hot rolling on the martensitic transformation of an equiatomic NiTi alloy. Suzuki et al. [18] have studied the hot ductility of a NiTi alloy by hot tensile test. They reported that a good hot ductility could be obtained for NiTi alloy within the temperature range of 900–1100 °C. In another research work, Frick et al. [3,19] have reported the delay in the formation of Ni rich precipitates and the occurrence of dynamic restoration processes during hot rolling of 50.9 at.% Ni–49.1 at.% Ti alloy within the temperature range of 845–950 °C with 50% thickness reduction. In a parallel work, McCormik [20] has shown that finished products for seismic application can be achieved by a combination of hot rolling and aging instead of hot rolling and cold rolling.

Recently, a number of studies have been carried out on the hot deformation of Ni rich NiTi alloys using hot compression test. Zhang et al. [21,22] have studied the flow behavior of 50.5 at.% Ni–49.5 at.% Ti and 50.7 at.% Ni–49.3 at.% Ti within the temperature range of 700–1000 °C. They have suggested a hyperbolic Sine equation to predict the flow stress of the alloys. In another research work, Dehghani and Khamei [23,24] have investigated the hot compression behavior of brittle NiTi alloy with the composition of 60 wt% Ni–40 wt% Ti (or 55 at.% Ni–45 at.% Ti) within the temperature range of 950–1050 °C and strain rate of  $0.001$ – $0.35 \text{ s}^{-1}$ . They have reported the occurrence of Dynamic Recrystallization, DRX. Besides, they have modeled the flow behavior of this alloy based on Zener–Holloman parameter,  $Z$ , in a hyperbolic Sine equation.

\* Corresponding author. Tel.: +98 21 77240540; fax: +98 21 77240480.

E-mail address: [kheirandish@iust.ac.ir](mailto:kheirandish@iust.ac.ir) (Sh. Kheirandish).

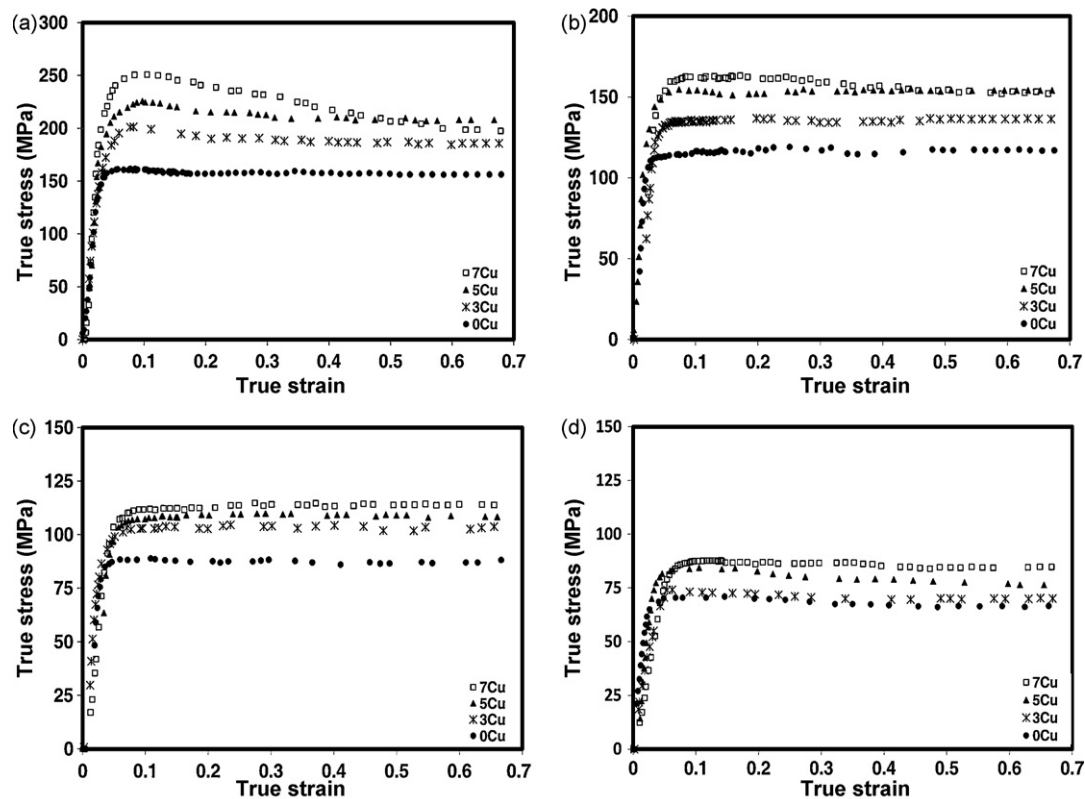


Fig. 1. Flow curves obtained for NiTi alloys with different Cu contents, at strain rate of  $0.1 \text{ s}^{-1}$  and different temperatures: (a)  $700^\circ\text{C}$ , (b)  $800^\circ\text{C}$ , (c)  $900^\circ\text{C}$ , and (d)  $1000^\circ\text{C}$ .

In spite of various studies conducted on the hot deformation of Ni rich NiTi alloys, to the best of authors' knowledge, few research work has been published on the hot compression behavior of near equiatomic binary NiTi and ternary NiTiCu alloys. Thus, the present work has been undertaken to investigate the hot deformation behavior of NiTi and NiTiCu alloys.

## 2. Materials and methods

The samples used in this study were made from ingots prepared by Vacuum Induction Melting (VIM) method with nominal composition of  $\text{Ti}_{50.4}\text{Ni}_{49.6-x}\text{Cu}_x$  ( $x=0, 3, 5, 7 \text{ at.}\%$ ). High purity pellets ( $\text{Ni} > 99.9 \text{ wt}\%$ ), Ti plates ( $\text{Ti} > 99.7 \text{ wt}\%$ ) and Cu wires ( $\text{Cu} > 99.98 \text{ wt}\%$ ) were used as raw materials. The furnace was evacuated to  $10^{-4}$  mbar and melting experiments were carried out on 250 g scale in a high-density graphite crucible. Homogenization heat treatment was conducted at  $1000^\circ\text{C}$  for 1 h. Cylindrical compression samples of 10 mm diameter and 15 mm height were prepared from the homogenized ingots. Compression tests were conducted over the temperature range of  $700\text{--}1000^\circ\text{C}$  at  $100^\circ\text{C}$  intervals and a constant strain rate of  $0.1 \text{ s}^{-1}$  by an Instron 8502 testing machine. The specimens were deformed under compression to a true strain of 0.7 and water cooled after deformation. The compressed specimens were sectioned parallel to the compression axis for microstructural examination and X-ray diffraction, XRD, analysis. The specimens were polished and etched in  $2\text{HF}\text{--}3\text{HNO}_3\text{--}1\text{H}_2\text{O}$ . Microstructures of specimens after the compression test were characterized by optical microscopy and Scanning Electron Microscopy, SEM. XRD analysis was carried out using  $\text{Cu K}\alpha$  radiation at  $30 \text{ kV}/100 \text{ mA}$  on samples deformed at  $800^\circ\text{C}$ . SEM equipped with micro analysis unit for Energy Dispersive Spectroscopy, EDS, was used to study the composition of phases.

## 3. Results and discussion

Flow curves of NiTi and NiTiCu alloys at various temperatures are shown in Fig. 1(a)–(d). The flow curves typically exhibit a gradual strain hardening at strains less than 0.1. The samples tested at lower temperatures show a peak stress followed by softening to an extensive steady state. While, above  $800^\circ\text{C}$  the softening behavior of flow curves is not represented clearly and steady state behavior can be seen.

This figure also shows that by increasing temperature, the peak stress falls. In addition, the shape of the flow curves vary by addition of Cu. It can be seen that the flow curves of NiTiCu alloys are obviously above that of NiTi alloy. Xujun et al. [25] have also stated in their research work that by addition of Cu to NiTi, the high temperature strength of this alloy increases.

Although the peak stress observed in flow curve is indicative of the occurrence of DRX, the onset of dynamic restoration processes cannot be identified from peak stress represented in flow curves. Ryan et al. [26] and Ploiak et al. [27] suggested that the onset of DRX entitled critical stress,  $\sigma_c$ , brings an inflection in the work hardening rate,  $\theta$ , versus stress,  $\sigma$ , curve; wherein  $\theta$  is the derivative of stress with respect to strain (i.e.  $\theta = \partial\sigma/\partial\varepsilon$ ).

Fig. 2(a) shows the variations of  $\theta$  versus  $\sigma$  for samples deformed at  $800^\circ\text{C}$ . As can be seen in this figure, in each curve  $\theta$  decreases rapidly by increasing flow stress probably due to the onset of dynamic recovery. Afterwards, the slope of the curves gradually decreases which shows the inflection point of the curves representing  $\sigma_c$ . Then the curves drop to  $\theta=0$  at peak stress. It should be noted that analysis of flow curves at  $700, 900$ , and  $1000^\circ\text{C}$  shows the same behavior, meaning that by increasing Cu content,  $\sigma_c$  shifts to higher amounts.

In order to determine an exact value of critical stress, Ploiak and Jonas [27] proposed that a null value of the derivative of work hardening rate with respect to stress,  $(-\partial\theta/\partial\sigma)$  is obtained at the critical stress. The critical stresses determined from plotting  $(-\partial\theta/\partial\sigma)$  versus  $\sigma$  for NiTi and NiTiCu alloys deformed at  $800^\circ\text{C}$  are shown in Fig. 2(b). As can be seen, these minimum points illustrate a good estimation of critical stresses which is confirmed by the results presented in Fig. 1 showing the increment of critical stress by increasing Cu content. This can be attributed to the formation of Cu containing phases caused by the substitution of Cu for Ni as shown in the XRD patterns of

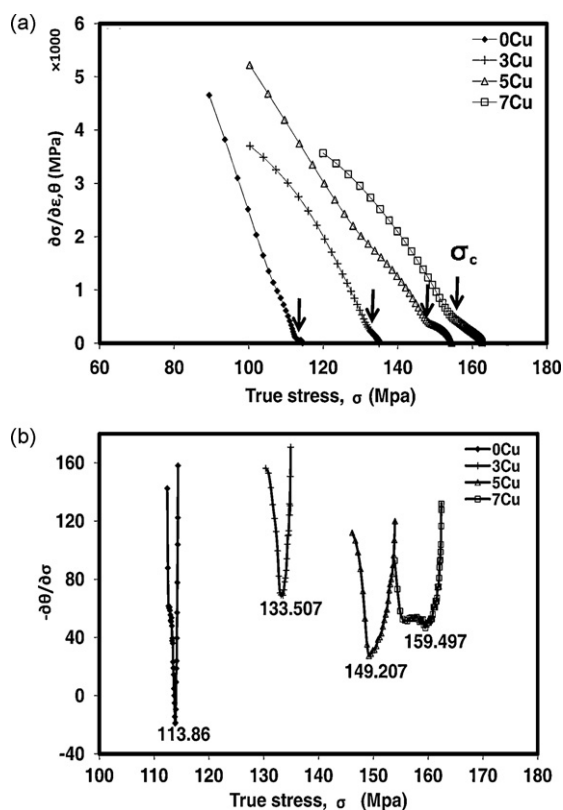


Fig. 2. (a) Work hardening rate versus flow stress and (b) factor of  $(-\partial\theta/\partial\sigma)$  as a function of  $\sigma$  at 800 °C for NiTi base alloys with different Cu contents.

binary NiTi and ternary NiTi5Cu samples deformed at 800 °C (Fig. 3).

However, because of oxygen contamination the oxide phases such as  $Ti_4Ni_2O$ ,  $Ti_4Cu_2O$  or  $Ti_4(Ni,Cu)_2O$  could also be formed. Since the crystallographic structure and lattice parameters of these oxides are almost the same as the relevant intermetallics, it is difficult to differentiate these phases and represent them in this work. This matter has also been reported by other researchers [28–32].

It is also believed that [28,33,34] Cu containing precipitates make the plasticity decrease but contribute to higher yield strength than achieved by  $Ti_2Ni$  precipitates. Thus, the presence of Cu containing precipitates would be effective in increasing the strength and decreasing the workability of NiTi alloy. Moreover, the XRD pattern of NiTiCu alloy reveals the solid solution of Cu in NiTi intermediate phase as it appeared in the form of  $TiNi_{0.8}Cu_{0.2}$  for the matrix.

SEM micrographs and EDS analysis of binary NiTi and NiTi5Cu alloys deformed at 800 °C obtained from the longitudinal section of samples are shown in Fig. 4. By comparing the micrographs presented in this figure one can see a eutectic kind of structure containing  $Ti_2Ni$  in binary NiTi alloy (marked A), while a typical precipitate containing Ti, Ni and Cu in ternary NiTi5Cu alloy (marked B) which is a complex compound of  $Ti_2Cu$  and  $Ti_2Ni$ , i.e.  $Ti_2(Ni,Cu)$  is present as well. The formation of this phase in NiTiCu alloys is also reported by Schuster et al. [35].

As can be seen in Fig. 4(e), the matrix of NiTi5Cu alloy contains 4.72 at.% Cu. The rest of Cu content is balanced with the precipitates containing 10.45 at.% Cu with approximate volume fraction of 1.5%. Therefore, a combination of precipitation and solid solution strengthening mechanisms causes the critical stress of the ternary alloys to increase.

Fig. 5 shows the variation of  $\theta$  versus  $\varepsilon$  for NiTi and NiTiCu alloys deformed at 800 °C. The maximum softening rate,  $\varepsilon^*$ , can

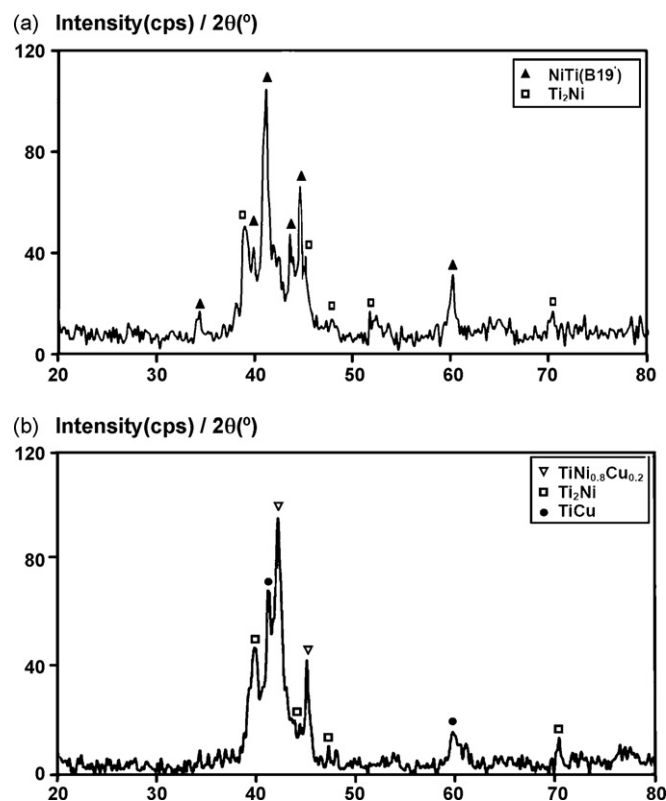


Fig. 3. XRD pattern of (a) NiTi and (b) NiTiCu alloys deformed at 800 °C.

be determined from the minima in  $\theta$ – $\varepsilon$  curves. As can be seen by increasing Cu content,  $\varepsilon^*$  shifts to higher values. This indicates that the addition of Cu can affect dynamic restoration processes. As mentioned above, solid solution hardening can be operative in NiTiCu alloys. By increasing Cu content, the effect of solute drag becomes more severe. Hence, the driving force for dynamic restoration processes will be increased by increasing of Cu content leading to the enhancement of the maximum softening rate.

The cross section of the samples deformed at 800 °C was studied by optical microscopy to analyze the microstructures shown in Fig. 6. The elongated and serrated grains (marked by arrows) can be readily observed in this figure. However, a few recrystallized grains are observed in the vicinity of grain boundaries. This implies that despite the applied strain of 0.7, the volume fraction of DRX grains is low in NiTi and NiTiCu alloys. Hence, Dynamic Recovery, DRV, is the dominant mechanism in these alloys and much higher strains are required for obtaining a nearly DRX microstructure. This behavior may also be attributed to high value of  $Z$ ; i.e. that the deformation temperature of 800 °C may be low for progression of DRX in these alloys.

In a similar work, Zhang et al. [21,22] obtained the same results. Moreover, the studies [36,37] carried out on the flow behavior of intermetallics with crystal structure similar to NiTi at high temperature (B2 structure), such as FeAl or  $Fe_3Al$  showed almost the same behavior. It means that flow softening type of curve was seen at low temperatures, while a steady state one was observed at high temperatures.

Comparison of the microstructure of alloys with different Cu content shows that the increase in Cu content results in the increase of volume fraction of Cu containing precipitates as well as the Cu content of solid solution. As mentioned before, this makes the critical stress of ternary alloys increase significantly as such increase in Cu content from 3 to 7 at.% causes the critical stress improvement by 30%.

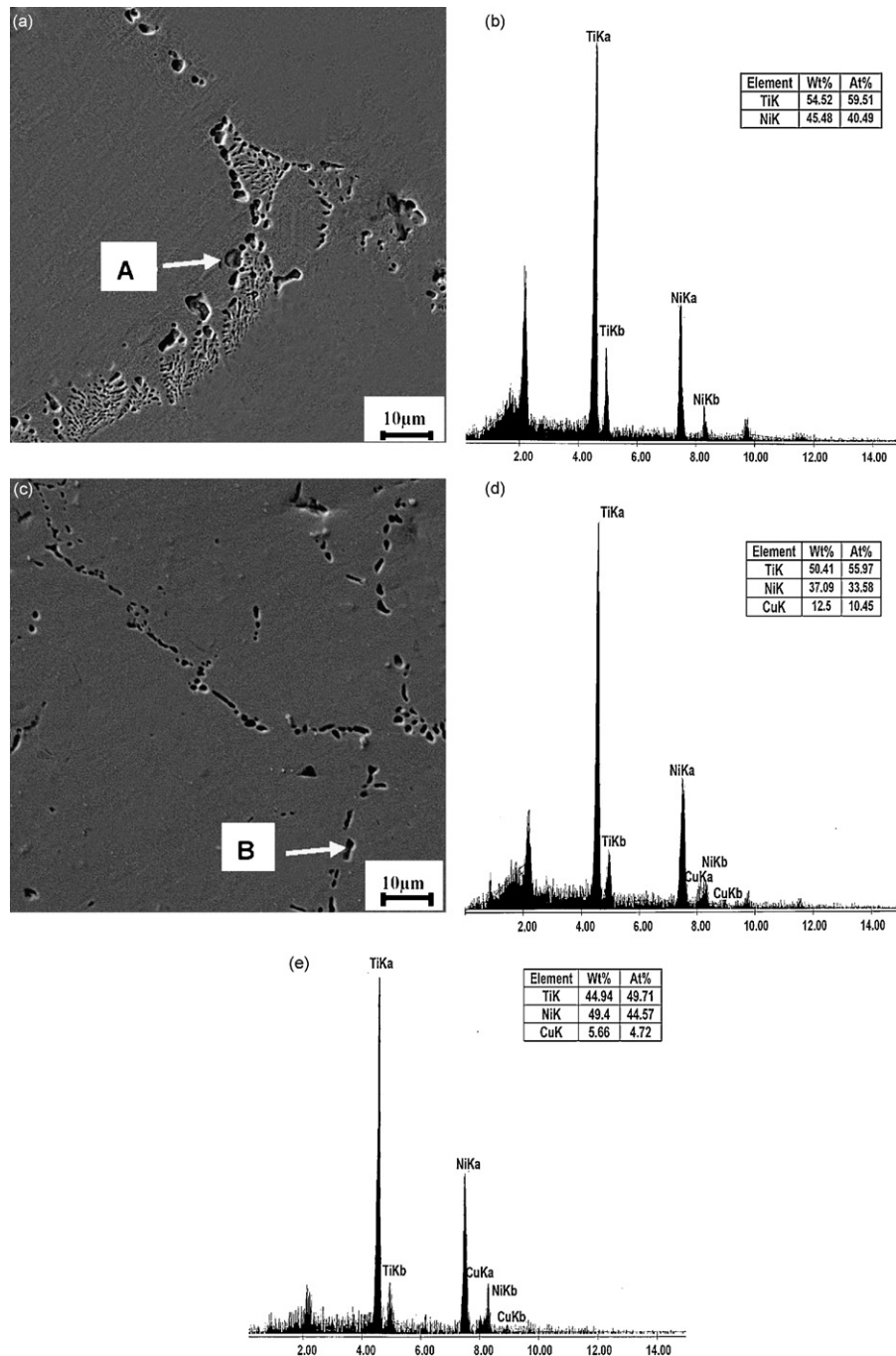


**Fig. 4.** SEM micrographs of alloys after hot deformation at 800 °C: (a) NiTi, (b) EDS analysis of the secondary phase marked A shown in (a), (c) NiTiCu, (d) EDS analysis of the secondary phase marked B, and (e) of the matrix shown in (c).

Moreover, this figure also shows that the stringers of the second phases were elongated in the direction perpendicular to the compression axis and the new DRX grains were not formed on these second phases. As can be seen in this figure, regardless of DRV mechanism, another mechanism followed by DRV, so called geometric dynamic recrystallization, GDRX, can be assumed to occur probably during hot deformation of these alloys. GDRX is a process by which a new grain structure is formed as a result of a change in grain geometry coupled with deformation. One prerequisite of complete GDRX is that the boundaries become serrated as a consequence of the interaction of subgrain boundaries with the existing grain boundaries. When the grains have thinned down

by deformation to the degree that the grain thickness reaches the grain boundary roughness, which is equal to twice the serration amplitude the serrations cause grain perforations. In this case, interpenetration of the serrated boundaries occurs, resulting in a microstructure of small equiaxed grains of a size comparable with the subgrain size [38–40]. According to Fig. 6, partial GDRX is found from pinching off of protrusion from few boundaries.

Typical microstructure of NiTi5Cu alloy deformed at higher temperature (1000 °C) is also shown in Fig. 7. One can see that by increasing temperature from 800 to 1000 °C, the grain size increases markedly, showing that the operative mechanism at 1000 °C is grain growth.



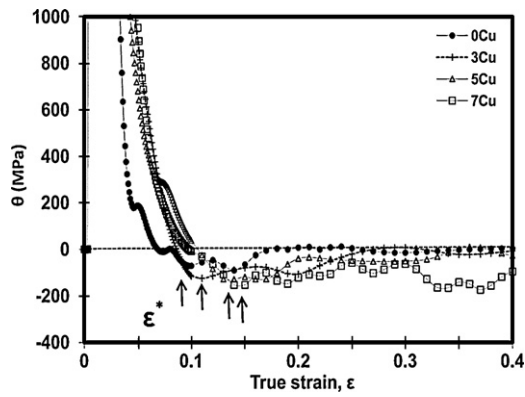


Fig. 5. Work hardening rate versus strain at 800 °C for NiTi based alloys with different Cu contents.

It is noticed that it is hard to predict the softening mechanism during hot deformation of NiTi alloys from the shape of the flow curves alone. This suggests that microstructural observation and other processing analyses are also necessary for determining the exact mechanism of dynamic restoration processes occurring in NiTi and NiTiCu alloys tested in this work.

#### 4. Conclusions

1. The increase in Cu content resulted in the increment of critical stress,  $\sigma_c$ , and the maximum softening rate,  $\varepsilon^*$ , determined based on the flow curves.

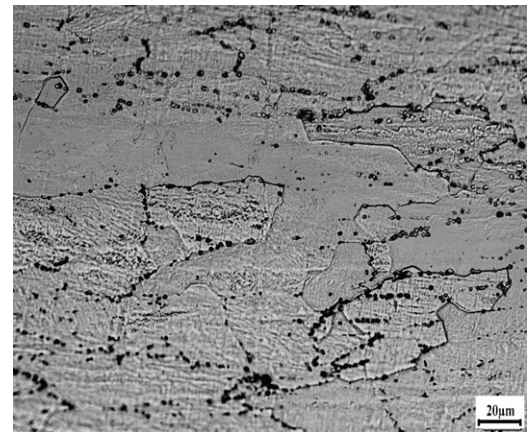


Fig. 7. Microstructure of NiTi5Cu deformed at 1000 °C.

2. A combination of precipitation and solid solution hardening played an effective role in the enhancement of flow stress in NiTiCu alloys.
3. The microstructure of samples deformed at 800 °C, consisted of serrated and elongated boundaries showing that DRV may be operative in NiTi and NiTiCu alloys. However, a few recrystallized grains found in the vicinity of those grain boundaries can be the evidence of DRX.
4. Microstructural analysis showed that grain growth was observed in NiTi5Cu alloy deformed at 1000 °C.

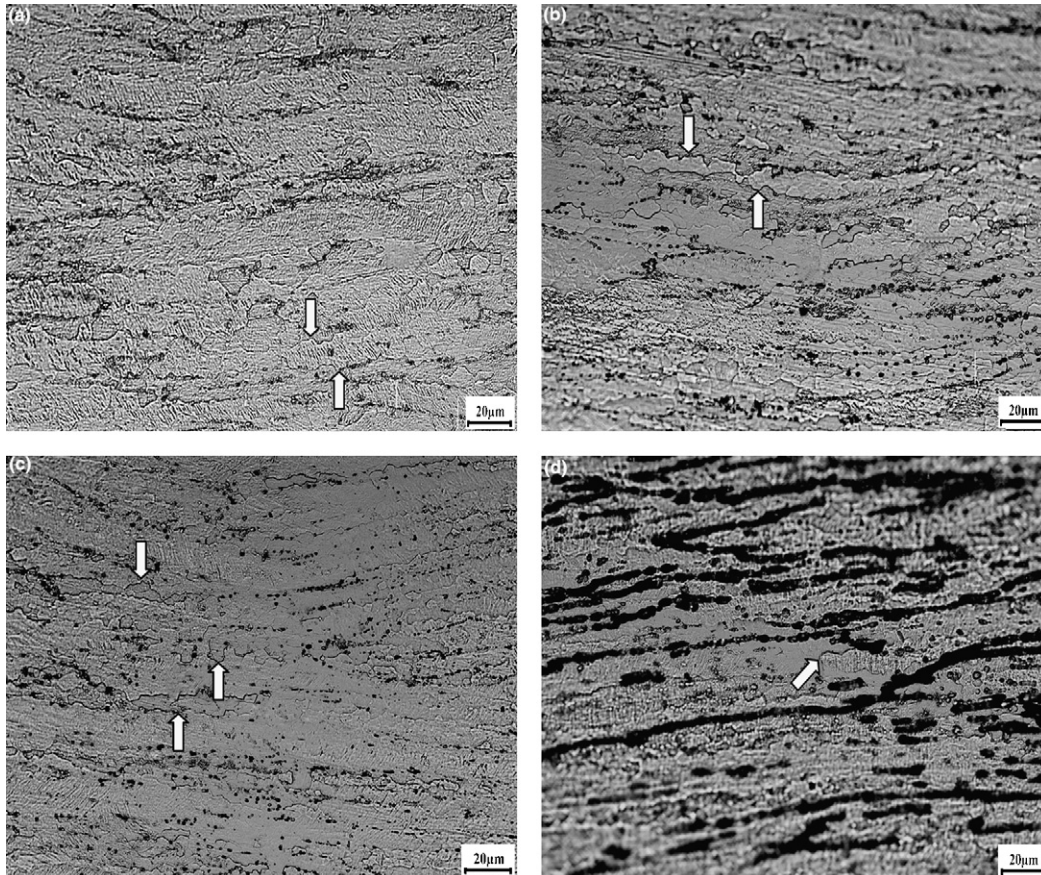


Fig. 6. Microstructures obtained under 800 °C for (a) NiTi, (b) NiTi3Cu, (c) NiTi5Cu, and (d) NiTi7Cu.

## References

- [1] K. Otsuka, X. Ren, *Progr. Mater. Sci.* 50 (2005) 511–678.
- [2] Z.G. Wei, R. Sandstrom, S. Miyazaki, *J. Mater. Sci.* 33 (1998) 3743–3762.
- [3] C.P. Frick, A.M. Ortega, J. Tyber, K. Gall, H.J. Maier, *Metall. Mater. Trans.* 35A (2004) 2013–2025.
- [4] G. Bozzolo, R.D. Noebe, H.O. Mosca, *J. Alloys Compd.* 389 (2005) 80–94.
- [5] Ch. Grossmann, J. Frenzel, V. Samphath, T. Depka, G. Eggeler, *Metall. Mater. Trans.* 40A (2009) 2531–2544.
- [6] F.J. Gil, E. Solano, J. Penal, E. Engel, A. Mendoza, J.A. Planell, *J. Mater. Sci. Mater. Med.* 15 (2004) 1181–1185.
- [7] W. Tang, R. Sandstrom, Z.G. Wei, S. Miyazaki, *Metall. Mater. Trans.* 31A (2000) 2423–2430.
- [8] S. Colombo, C. Cannizzo, F. Gariboldi, G. Airolidi, *J. Alloys Compd.* 422 (2006) 313–320.
- [9] N.N. Popov, S.D. Prokoshkin, M.Yu. Sidorkin, T.I. Sysoeva, D.V. Borovkov, A.A. Aushev, I.V. Kostylev, A.E. Gusarov, *Russ. Metall. (Metally)* 1 (2007) 59–64.
- [10] A.S. Paula, K.K. Mahesh, F.M.B. Fernandes, *Eur. Phys. J. Spec. Top.* 158 (2008) 45–51.
- [11] I. Karaman, H. Ersin Karaca, H.J. Maier, Z.P. Luo, *Metall. Mater. Trans.* 34A (2003) 2527–2539.
- [12] A.S. Paula, K.K. Mahesh, C.M.L.D. Santos, F.M.B. Fernandes, C.S.D.C. Viana, *Mater. Sci. Eng.* 481–482A (2007) 146–150.
- [13] B. Kockar, I. Karaman, A. Kulkarni, Y. Chumlyakov, I.V. Kireeva, *J. Nucl. Mater.* 361 (2007) 298–305.
- [14] T. Kurita, H. Matsumoto, H. Abe, *J. Alloys Compd.* 381 (2004) 158–161.
- [15] S.K. Sadrnezhaad, S.H. Mirabolghasemi, *Mater. Des.* 28 (2007) 1945–1948.
- [16] R. Kocich, M. Kursá, M. Greger, I. Szurman, *Acta Metall. Slovaca* 13 (2007) 570–579.
- [17] H.C. Lin, S.K. Wu, *Mater. Sci. Eng.* 158A (1992) 87–91.
- [18] H.G. Suzuki, E. Takakura, D. Eylon, *Mater. Sci. Eng.* 263A (1999) 230–236.
- [19] C.P. Frick, A.M. Ortega, J. Tyber, A.El.M. Maksound, H.J. Maier, Y. Liu, K. Gall, *Mater. Sci. Eng.* 405A (2005) 34–39.
- [20] J.P. McCormick, Ph.D. Thesis, Georgia Institute of Technology (2006).
- [21] W. Zhang, S. Zang, *Acta Metall. Sin.* 42 (2006) 1036–1040.
- [22] H. Zhang, Y. He, X. Liu, J. Xie, *Acta Metall. Sin.* 43 (2007) 930–936.
- [23] K. Dehghani\*, A.A. Khamei, *Mater. Sci. Eng.* 527A (2010) 684–690.
- [24] A.A. Khamei, K. Dehghani, *J. Alloys Compd.* (2009), doi:10.1016/j.jallcom.2009.09.187.
- [25] M. Xujun, G. Jinfang, Z. Ming, Development of a TiNiCu shape memory alloy, in: *Shape Memory Materials'94—Proceeding*, 1994, pp. 220–224.
- [26] N.D. Ryan, H.J. McQueen, *J. Mater. Proc. Technol.* 20 (1990) 177–199.
- [27] E.I. Poliak, J.J. Jonas, *ISIJ Int.* 43 (2003) 684–691.
- [28] W.J. Moberley, Ph.D. Thesis, Stanford University (1991).
- [29] H.C. Lin, S.K. Wu, J.C. Lin, *Mater. Chem. Phys.* 37 (1994) 184–190.
- [30] S.K. Wuy, J.J. Su, J.Y. Wang, *Philos. Mag.* 84 (12) (2004) 1209–1218.
- [31] H. Luo, F. Shan, Y. Huo, Y. Wang, *Thin Solid Films* 339 (1999) 305–308.
- [32] V.G. Chuprina, I.M. Shalya, *Powder Metall. Met. Ceram.* 41 (2002) 85–89.
- [33] F. Gao, H.M. Wang, *Intermetallics* 16 (2008) 202–208.
- [34] Z.Y. Suo, K.Q. Qiu, Q.F. La, Y.L. Ren, Z.Q. Hu, *J. Alloys Compd.* 463 (2008) 564–568.
- [35] J.C. Schuster, G. Cacciamani, *Light Metal Ternary Systems: Phase Diagrams, Crystallographic and Thermodynamic Data*, in: Landolt-Börnstein-Group 5 Phys. Chem., vol. 11A4, Springer, Berlin/Heidelberg, 2006.
- [36] D. Kuc, G. Niewielski, I. Bednarczyk, *J. Achieve. Mater. Manuf. Eng.* 18 (2008) 123–130.
- [37] M. Jablonska, K. Rodak, G. Niewielski, *J. Achieve. Mater. Manuf. Eng.* 29 (2006) 107–110.
- [38] F.J. Humphreys, M. Hatherly, *Recrystallization and Related Annealing Phenomena*, second ed., Elsevier Ltd., UK, 2004.
- [39] W. Blum, Q. Zhu, R. Merke, H.J. McQueen, *Mater. Sci. Eng.* 205A (1996) 23–30.
- [40] H.J. McQueen, W. Blum, *Mater. Sci. Eng.* 290A (2000) 95–107.